

Equation of state in the pion condensation phase in the asymmetric nuclear matter using a holographic QCD model

Hiroki Nishihara^{*1} and Masayasu Harada^{†1}

¹ *Department of Physics, Nagoya University, Nagoya 464-8602, Japan*

(Dated: October 21, 2014)

We study the asymmetric nuclear matter using a holographic QCD model by introducing a baryonic charge in the infrared boundary. We first show that, in the normal hadron phase, the predicted values of the symmetry energy and its slope parameter are comparable with the empirical values. We find that the phase transition from the normal phase to the pion condensation phase is delayed compared with the pure mesonic matter: The critical chemical potential is larger than the pion mass which is obtained for the pure mesonic matter. We also show that, in the pion condensation phase, the pion contribution to the isospin number density increases with the chemical potential, while the baryonic contribution is almost constant. Furthermore, the value of chiral condensation implies that the enhancement of the chiral symmetry breaking occurs in the asymmetric nuclear matter as in the pure mesonic matter. We also give a discussion on how to understand the delay in terms of the 4-dimensional chiral Lagrangian including the rho and omega mesons based on the hidden local symmetry.

PACS numbers: 11.25.Tq, 11.30.Rd, 21.65.Cd, 21.65.Mn

I. INTRODUCTION

It is expected that investigation of the hadron physics in extreme conditions will give a clue for our understanding of QCD (Quantum Chromodynamics). In particular studying asymmetric nuclear matter is also important to derive the equation of state inside neutron stars [1], which will give a clue to understand the recently found very heavy neutron star [2, 3].

We often draw the QCD phase diagram on the plane of temperature T and the baryon chemical potential μ_B [4, 5]. It is expected that various phases exist on the plane (T, μ_B) of the phase diagram: e.g. the quark-gluon plasma phase and the color superconducting phase. Similarly, finite isospin chemical potential μ_I provide a rich phase structure which includes the pion condensation phase. There are many works studying the phase diagram at $\mu_I \neq 0$. In particular, the pion condensation phase transition on the plane (μ_B, μ_I) are studied by introducing μ_I together with μ_B in the Nambu-Jona-Lasinio (NJL) model [6–15] and holographic QCD models [16, 17] and so on [18–21].

As a first step to study the rich phase structure, it is interesting to study the phase transition from the normal hadron phase to the pion condensation phase together with the equation of state in the pion condensation phase on the plane (μ_B, μ_I) . References [6–11] show the $T - \mu_B - \mu_I$ phase diagram via the NJL model, in which the dependence of the isospin density on the isospin chemical potential is shown only for $T = \mu_B = 0$. On the other hand, by using holographic QCD models [16, 17], the pion condensation phase transition is discussed. In Ref. [17],

they draw the phase diagram on the plane (μ_B, μ_I) in the Sakai-Sugimoto model. Reference [16] also studies stability of the normal hadron phase at finite isospin density by introducing the baryon charge as the Reissner-Nordström (RN) blackhole charge in a hard wall holographic QCD model. However, the equation of state in the pion condensation phase is not discussed in these works.

In the previous work [22], we studied the pion condensation in the pure mesonic matter using a holographic QCD model by introducing the isospin chemical potential as a UV boundary value of the gauge field. We showed that the phase transition from the normal hadron phase to the pion condensation phase is of the second order and the critical value of the isospin chemical potential is equal to the pion mass, consistently with the chiral Lagrangian analysis [23].

In Ref. [22], we studied the μ_I -dependence of the chiral condensate defined by $\tilde{\sigma} \equiv \sqrt{\langle \sigma \rangle^2 + \langle \pi^a \rangle^2}$, and showed that, although the “ σ ”-condensate decreases rapidly with the isospin chemical potential in the pion condensation phase, the π -condensate increases more rapidly. As a result the chiral condensate $\tilde{\sigma}$ keeps increasing, which implies the enhancement of the chiral symmetry breaking in the pion condensation phase. The symmetry structure for this is understood in the following way: When the isospin chemical potential is introduced, the chiral symmetry $SU(2)_R \times SU(2)_L$ is explicitly broken to $U(1)_R^{(3)} \times U(1)_L^{(3)} = U(1)_V^{(3)} \times U(1)_A^{(3)}$, where the superscript (3) implies that the generator T_3 of $SU(2)$ is used for the $U(1)$ as $\exp[i\theta_V T_3] \in U(1)_V^{(3)}$. In the normal hadron phase the $U(1)_A^{(3)}$ is broken by the “ σ ”-condensate spontaneously and the quark mass explicitly. In the pion condensation phase, on the other hand, the $U(1)_V^{(3)}$ symmetry is spontaneously broken by the π -condensate, which generates a massless Nambu-Goldstone boson. Since both $U(1)_A^{(3)}$ and $U(1)_V^{(3)}$ are

^{*}h248ra@hken.phys.nagoya-u.ac.jp

[†]harada@hken.phys.nagoya-u.ac.jp

subgroups of the chiral $SU(2)_R \times SU(2)_L$ symmetry, the above structure implies that the chiral symmetry is never restored in the mesonic matter with the isospin chemical potential, and actually the breaking is enhanced in the pion condensation phase. We note that the above properties are obtained in the pure mesonic matter, so that it is interesting to ask whether they are changed by the existence of the nucleon in the matter.

In this paper, we adopt a simple way for introducing the baryonic sources: We include a point-like nucleon source at the IR boundary coupling to the iso-triplet vector meson in the hard wall holographic QCD model as in Ref. [24], and studied the pion condensation in the asymmetric nuclear matter. We will show that the phase transition from the normal hadron phase to the pion condensation phase is delayed in the asymmetric nuclear matter compared with the pure mesonic matter. In other words, the critical chemical potential is larger than the pion mass. On the other hand, the enhancement of the chiral symmetry breaking still occurs since the chiral condensate $\tilde{\sigma}$ keeps increasing with the isospin chemical potential.

This paper is organized as follows: In section II, we briefly review the holographic QCD model used in our analysis, and introduce the baryonic charge following Ref. [24]. Section III is devoted to the study of the symmetry energy and the pion mass in the normal hadron phase. In section IV, we study the pion condensation phase and obtain the relation between the isospin chemical potential and the isospin number density as well as the chiral condensate. In section V, we make an analysis of the pion mass in the normal hadron phase using the four dimensional chiral model based on the hidden local symmetry [25, 26]. We give a summary and discussions in section VI. We also show the equations of motion in appendix A.

II. MODEL

In the present analysis, we employ a holographic QCD model given in Refs. [27–29] for the mesonic part. Then the mesonic action in the five dimensional space is given by

$$S_5 = S_X + S^{\text{BD}} \quad (\text{II.1})$$

where

$$S_X = \int d^4x \int_{\epsilon}^{z_m} dz \sqrt{g} \text{Tr} \left\{ |DX|^2 - m_5^2 |X|^2 - \frac{1}{4g_5^2} (F_L^2 + F_R^2) \right\}, \quad (\text{II.2})$$

$$S^{\text{BD}} = - \int d^4x \int_{\epsilon}^{z_m} dz \sqrt{g} \text{Tr} \{ \lambda z_m |X|^4 - m^2 z_m |X|^2 \} \delta(z - z_m) \quad (\text{II.3})$$

with $m_5^2 = -3$. The metric is written as

$$ds^2 = a^2(z) (\eta_{\mu\nu} dx^\mu dx^\nu - dz^2) = g_{MN} dx^M dx^N \quad (\text{II.4})$$

with

$$a(z) = \frac{1}{z}, \quad (\text{II.5})$$

where z_m and ϵ are the IR-cutoff and UV-cutoff. Here N and M run over 0,1,2,3,5 and $\eta_{\mu\nu}$ is the defined as the Minkowski metric: $\eta_{\mu\nu} = \text{diag}(1, -1, -1, -1)$.¹

The model has the chiral symmetry $U(2)_L \times U(2)_R$ ($= U(1)_L \times U(1)_R \times SU(2)_L \times SU(2)_R$), under which the fields transform in the following form:

$$X \rightarrow X' = g_L X g_R^\dagger, \quad (\text{II.6})$$

$$L_M \rightarrow L'_M = g_L L_M g_L^\dagger + i g_L \partial_M g_L^\dagger, \quad (\text{II.7})$$

$$R_M \rightarrow R'_M = g_R R_M g_R^\dagger + i g_R \partial_M g_R^\dagger \quad (\text{II.8})$$

with $g_R \in U(2)_R$ and $g_L \in U(2)_L$. The covariant derivative and the field strength are defined as

$$D_M X = \partial_M X - i L_M X + i X R_M, \quad (\text{II.9})$$

$$F_{MN}^L = \partial_M L_N - \partial_N L_M - i [L_M, L_N] \quad (\text{II.10})$$

and similar for F_{MN}^R . These fields are parametrized as

$$L_M^I = \text{Tr} [L_M \sigma^I], \quad R_M^I = \text{Tr} [R_M \sigma^I], \quad (\text{II.11})$$

$$V_M^I = \frac{R_M^I + L_M^I}{2}, \quad A_M^I = \frac{R_M^I - L_M^I}{2}, \quad (\text{II.12})$$

$$X = \frac{1}{2} (\sigma^0 \sigma^0 + S^a \sigma^a) e^{i\pi^b \sigma^b + i\eta} \quad (\text{II.13})$$

where $\sigma^I = (\sigma^0, \sigma^a) = (1, \sigma^a)$ and σ^a are the Pauli matrices. In the following analysis we adopt the gauge $L_5 = R_5 = 0$ and the IR boundary condition $F_{5\mu}^L|_{z_m} = F_{5\mu}^R|_{z_m} = 0$.

Now, let us include the effects of the nucleon into the model. Here we introduce baryonic sources for the quark number density n_q and the baryonic contribution to the isospin number density, denoted by n_I^{Baryon} , through the following term²:

$$S_{\text{int}} = \int d^4x \int_{\epsilon}^{z_m} dz \left[V_0^0 n_q + V_0^3 n_I^{\text{Baryon}} \right] \delta(z - z_m + \delta z) \quad (\text{II.14})$$

where δz (> 0) is an infinitesimal length and V_0^0 and V_0^3 are the gauge fields corresponding to the quark number density and isospin number density. The baryon number

¹ Although there is a Chern-Simons term in addition, the term does not affect our result since we assume the rotational invariance in the present analysis.

² The sign of this term is uniquely determined from the definition of the chemical potential introduced in Eq. (II.16).

density n_B is defined as $n_B = n_q/N_c$. We introduced the baryonic sources by the δ -function having a peak near the IR boundary [24], which doesn't modify the IR boundary conditions.

In the present analysis, we assume that the proton (neutron) does not appear as long as the proton (neutron) chemical potential μ_p (μ_n) is smaller than the mass of a nucleon, denoted by m_N . Therefore our analysis will be done for the following three cases separately:

$$\begin{aligned} \text{(i)} \quad & -m_N \leq \mu_p < m_N, \quad -m_N \leq \mu_n < m_N, \\ \text{(ii)} \quad & m_N \leq \mu_p, \quad -m_N \leq \mu_n < m_N, \\ \text{(iii)} \quad & m_N \leq \mu_p, \quad m_N \leq \mu_n. \end{aligned} \quad (\text{II.15})$$

The proton and neutron chemical potential μ_p and μ_n are related with the isospin chemical potential μ_I and the baryon chemical potential μ_B through $\mu_p = \mu_B + \mu_I/2$ and $\mu_n = \mu_B - \mu_I/2$. The assumption implies $2n_I^{\text{Baryon}} = n_B = 0$ in Case-(i) and $2n_I^{\text{Baryon}} = n_B = n_p$ in Case-(ii) because n_I^{Baryon} and n_B are expressed as the difference between the proton density n_p and the neutron density n_n and the sum of them, respectively: $n_I^{\text{Baryon}} = \frac{n_p - n_n}{2}$, $n_B = n_p + n_n$. Case-(i) corresponds to the pure mesonic case which is studied in Ref. [22]. On the other hand, n_I^{Baryon} and n_B are independent of the each other in Case-(iii). We will show the results of our analysis in the Case-(ii) and the Case-(iii) to compare with the pure mesonic case.

We note that the four-dimensional part of the gauge symmetry is fixed when S_{int} is introduced. In other words, S_{int} is not invariant under the four-dimensional gauge transformation. Then, we introduce the quark number chemical potential μ_q and the isospin chemical potential μ_I as the UV boundary values of the time components of the gauge fields as ³

$$V_0^0|_\epsilon = \mu_q - c_{(0)}, \quad V_0^3|_\epsilon = \mu_I - c_{(3)}, \quad (\text{II.16})$$

where the constants $c_{(0)}$ and $c_{(3)}$ are corresponding to the degree of freedom of the gauge transformation. In the next section, we will determine the values of $c_{(0)}$ and $c_{(3)}$ by the physical requirements for the pion mass and the equation of state between the chemical potential and the density.

This holographic QCD model involves the following five parameters,

$$g_5^2, \quad z_m, \quad m_q, \quad \lambda, \quad m^2. \quad (\text{II.17})$$

To match this model with QCD, the parameter g_5^2 is adjusted as [27]

$$\frac{1}{g_5^2} = \frac{N_c}{12\pi^2}. \quad (\text{II.18})$$

For the physical inputs to determine the parameters, we use the pion mass $m_\pi = 139.6\text{MeV}$, the pion decay constant $f_\pi = 92.4\text{MeV}$, the ρ meson mass $m_\rho = 775.8\text{MeV}$, and the a_0 meson mass. As in Ref. [22], we use the a_0 meson mass $m_{a_0} = 980\text{MeV}$ as a reference value, and see the dependence of our results on the scalar meson mass. The values of the parameters corresponding to $m_{a_0} = 980\text{MeV}$ are determined as

$$\begin{aligned} z_m &= 1/(323\text{MeV}), \quad m_q = 2.29\text{MeV}, \\ \lambda &= 4.4, \quad m^2 = 5.39. \end{aligned} \quad (\text{II.19})$$

As in Ref. [22], we assume that the pion condensation phase has the rotational symmetry, $L_i = R_i = 0$ ⁴, and the iso-triplet scalars do not condense, $S^a = 0$. Furthermore, we take $V_0^1 = V_0^2 = 0$ and $A_0^3 = \pi^3 = 0$ which form a set of solutions of the equation of motion (EOM) for these fields. Similarly, the set of the $\eta = 0$ and $A_0^0 = 0$ satisfies the EOM and we take this solution.

The grand potential density Ω is given from the Lagrangian \mathcal{L} :

$$\Omega = - \int_\epsilon^{z_m} dz \mathcal{L} \quad (\text{II.20})$$

where the explicit form of the Lagrangian \mathcal{L} is shown in Eq. (A.2). One can derive the EOM for the vector field V_0^0 and V_0^3 from Eq. (II.20),

$$\begin{aligned} \partial_5 \frac{a}{g_5^2} \partial_5 V_0^0 &= n_q \delta(z - z_m + \delta z), \\ \partial_5 \frac{a}{g_5^2} \partial_5 V_0^3 - \frac{a^3 (S^0)^2}{2} [2 \sin^2 b V_0^3 + \theta \sin 2b \sin \zeta] \\ &= n_I^{\text{Baryon}} \delta(z - z_m + \delta z). \end{aligned} \quad (\text{II.21})$$

By parameterizing V_0^0 and V_0^3 as

$$\begin{aligned} V_0^0(z) &= \mu_q - c_{(0)} + \varphi^0(z) + g_5^2 n_q \int_\epsilon^z d\tilde{z} \tilde{z} \theta(\tilde{z} - z_m + \delta z), \\ V_0^3(z) &= \mu_I - c_{(3)} + \varphi^3(z) + g_5^2 n_I^{\text{Baryon}} \int_\epsilon^z d\tilde{z} \tilde{z} \theta(\tilde{z} - z_m + \delta z) \end{aligned} \quad (\text{II.22})$$

where θ is a step function, Eq. (II.21) is rewritten as

$$\begin{aligned} \partial_5 \frac{a}{g_5^2} \partial_5 \varphi^0 &= 0, \\ \partial_5 \frac{a}{g_5^2} \partial_5 \varphi^3 &= \frac{a^3 (S^0)^2}{2} [2 \sin^2 b (\mu_I - c_{(3)} + \varphi^3) \\ &\quad + \theta \sin 2b \sin \zeta]. \end{aligned} \quad (\text{II.23})$$

³ The baryon number chemical potential μ_B is related to μ_q as $\mu_B \equiv N_c \mu_q$.

⁴ Note that we also take expectation values of operators made by L_i and R_i such as $\sum_i R_i R_i$, which are invariant under the rotational symmetry, vanish since our present analysis is of the leading order in the large N_c expansion and the hadronic loop contributions are suppressed.

Here the boundary conditions are given by

$$\begin{aligned} V_0^{(0,3)} \Big|_{\epsilon} &= \mu_{(q,I)} - c_{(0,3)} , \quad \partial_5 V_0^{(0,3)} \Big|_{z_m} = 0 \\ \rightarrow \quad \varphi^{(0,3)} \Big|_{\epsilon} &= 0 , \quad \begin{cases} \partial_5 \varphi^0 \Big|_{z_m} = -g_5^2 z_m n_q \\ \partial_5 \varphi^3 \Big|_{z_m} = -g_5^2 z_m n_I^{\text{Baryon}} \end{cases} . \end{aligned} \quad (\text{II.24})$$

III. SYMMETRY ENERGY AND DELAY OF THE PHASE TRANSITION

In this section we first study the dependence of the pion mass on the isospin chemical potential μ_I in the normal hadron phase to show the delay of the pion condensation compared with the pure mesonic matter studied in Ref. [22]. Next, we investigate the symmetry energy to check whether the present way to introduce the baryonic matter works well in the normal hadron phase by comparing our result with its empirical value. For studying the hadron phase we set $b = 0$ and $\theta = 0$ in the equations of motion in Eqs. (II.21) and (II.23).

In Case-(iii), we first derive the relation between the chemical potential μ_I and the isospin number density n_I . For $b = \theta = 0$, it is easy to solve the equation of motion (II.23) with the boundary conditions in Eq. (II.24) to have

$$\varphi^3 = -\frac{g_5^2 n_I^{\text{Baryon}}}{2} z^2 . \quad (\text{III.1})$$

Substituting this solution into Eq. (II.20), we obtain

$$\begin{aligned} \Omega \supset & - \int_{\epsilon}^{z_m} dz \frac{a}{2g_5^2} (\partial_5 V_0^3)^2 - n_I^{\text{Baryon}} V_0^3 \Big|_{z_m - \delta z} \\ & = \frac{g_5^2 z_m^2}{4} (n_I^{\text{Baryon}})^2 - (\mu_I - c_{(3)}) n_I^{\text{Baryon}} \end{aligned} \quad (\text{III.2})$$

where $a = \frac{1}{z}$. Minimizing the Ω in terms of the n_I^{Baryon} for a given value of the isospin chemical potential μ_I yields the relation between the isospin chemical potential μ_I and the isospin number density of the asymmetric matter n_I^{Baryon} :

$$n_I^{\text{Baryon}} = \frac{2}{g_5^2 z_m^2} (\mu_I - c_{(3)}) . \quad (\text{III.3})$$

Here in the normal hadron phase the isospin density n_I equals to the density n_I^{Baryon} because mesons carrying isospin charge do not condense.

Similarly, for the quark number density we also have

$$n_q = \frac{2}{g_5^2 z_m^2} (\mu_q - c_{(0)}) . \quad (\text{III.4})$$

The baryon number density, $n_B = n_q/N_c$, appears when the baryon chemical potential μ_N is larger than the mass of nucleon $m_N = 939\text{MeV}$. This implies that the $c_{(0)}$

is determined as $c_{(0)} = m_N/N_c$, as in Ref. [24]. This argument yields the following relation:

$$n_B = \frac{2}{g_5^2 z_m^2 N_c^2} (\mu_B - m_N) . \quad (\text{III.5})$$

Let us next study the μ_I -dependence of the pion mass. The equations of motion for the pion fluctuation up till the quadratic order in the momentum space are given by

$$\begin{aligned} -\frac{1}{a(aS^0)^2} \partial_5 \left[a(aS^0)^2 \partial_5 \pi^{\pm} \right] &= E^{\pm}(\mu_I) [A_0^{\pm} + \pi^{\pm} E^{\pm}(\mu_I)] , \\ \frac{1}{a(aS^0)^2} \partial_5 \left(\frac{a}{g_5^2} \partial_5 A_0^{\pm} \right) &= [A_0^{\pm} + \pi^{\pm} E^{\pm}(\mu_I)] \end{aligned} \quad (\text{III.6})$$

where the fields are parameterized as

$$\pi^{\pm} = \frac{\pi^1 \mp i\pi^2}{\sqrt{2}} , \quad A_0^{\pm} = i \frac{A_0^1 \mp iA_0^2}{\sqrt{2}} \quad (\text{III.7})$$

and

$$E^{\pm}(\mu_I) = M \pm \mu_I \left(1 - \frac{z^2}{z_m^2} \right) \mp c_{(3)} \frac{z^2}{z_m^2} . \quad (\text{III.8})$$

S^0 is the solution of Eq. (A.1) and M is the energy of the static pion. Equation (III.6) together with the boundary conditions, $\pi|_{\epsilon} = \partial_5 \pi|_{z_m} = 0$, yield the value of the M as the eigenvalue. The lowest value of the eigenvalue M is identified with the pion mass, m_{π}^* . Here the parameter $c_{(3)}$ is determined as zero by assuming that π^+ and π^- are degenerating at $\mu_I = 0$: $E^{\pm}(\mu_I) = M \pm \mu_I (1 - z^2/z_m^2)$.

Figure 1 shows the μ_I dependence of the pion mass in the normal hadron phase. The π^- mass drawn by the red curve increases with the isospin chemical potential. The π^+ mass by the green curve, on the other hand, decreases and reaches zero at $\mu_I = 235\text{MeV}$, which implies that the π^+ condenses and that the transition to the pion condensation phase occurs. We would like to stress that the π^+

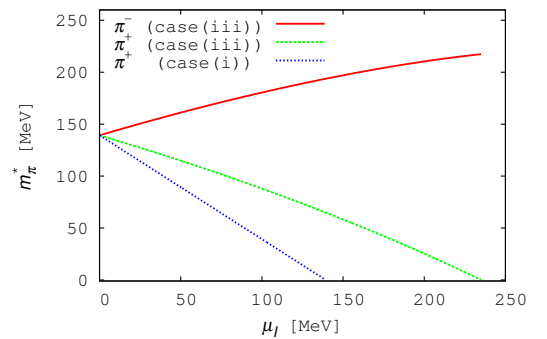


Fig. 1: μ_I dependence of the pion masses. The red and green curves show the masses of π^- and π^+ , respectively. We also show the μ_I dependence of the π^+ mass in the pure mesonic matter obtained in Ref. [22] by the blue curve.

mass here decreases more slowly than the one obtained in

the pure mesonic matter shown by the blue curve. One can easily see that the critical value of the isospin chemical potential for the phase transition is larger than the pion mass for the pure mesonic case. This is due to the existence of the baryons in the matter, which can also be understood by an analysis of the chiral Lagrangian based on the Hidden Local Symmetry as shown in section V.

The energy density of the system is defined as $\mathcal{E} = \Omega + n_q \mu_q + n_I \mu_I$ at zero temperature and given by

$$\mathcal{E} = \frac{g_5^2 z_m^2}{4} (n_I)^2 + \frac{g_5^2 z_m^2 N_c^2}{4} (n_B)^2. \quad (\text{III.9})$$

Then, the symmetry energy is obtained as ⁵

$$E_{\text{sym}}(n_B) \equiv \left. \frac{\partial(\mathcal{E}/n_B)}{\partial \alpha^2} \right|_{\alpha=0} = \frac{g_5^2 z_m^2}{16} n_B \quad (\text{III.10})$$

where $\alpha \equiv \frac{2n_I}{n_B}$. At the saturation density $n_0 = 0.16 \text{ fm}^{-3}$, we can estimate $E_{\text{sym}}(n_0) = 29 \text{ MeV}$ by using Eq. (II.18) and Eq. (II.19), which is comparable to the empirical value of $32.3 \pm 1.0 \text{ MeV}$ [31]. In Refs. [32, 33], the value of the parameter γ defined as $E_{\text{sym}}(n_B) = E_{\text{sym}}(\rho_0) \left(\frac{n_B}{n_0} \right)^\gamma$ is estimated as $\gamma = 0.55 - 0.69$, which is different from the result of the present analysis, $\gamma = 1$. The slope parameter of the symmetry energy is given by

$$L \equiv 3n_0 \left. \frac{\partial E_{\text{sym}}(n_B)}{\partial n_B} \right|_{n_B=n_0} = 3n_0 \frac{g_5^2 z_m^2}{16} \quad (\text{III.11})$$

and its value is estimated as $L = 87 \text{ MeV}$, where its empirical value is known as $45.2 \pm 10.0 \text{ MeV}$ [31]. We may understand that the deviations of values of γ and L are caused by the next leading order in the large N_c expansion.

In Case-(ii), as we stated in section II, $2n_I^{\text{Baryon}}$ and n_B are equal to n_p , which leads to the following solutions of Eq. (II.23) in the normal hadron phase, $b = \theta = 0$:

$$\begin{aligned} \varphi^3 &= -\frac{g_5^2 n_I^{\text{Baryon}}}{2} z^2 = -2\frac{g_5^2 n_p}{2} z^2, \\ \varphi^0 &= -\frac{g_5^2 n_q}{2} z^2 = -N_c \frac{g_5^2 n_p}{2} z^2. \end{aligned} \quad (\text{III.12})$$

Now, the grand potential density is given by

$$\begin{aligned} \Omega &\supset - \int_{\epsilon}^{z_m} dz \frac{a}{2g_5^2} \left[(\partial_5 V_0^0)^2 + (\partial_5 V_0^3)^2 \right] \\ &\quad - n_I^{\text{Baryon}} V_0^3 \Big|_{z_m - \delta z} - n_q V_0^0 \Big|_{z_m - \delta z} \\ &= \frac{g_5^2}{4} \left(N_c^2 + \frac{1}{4} \right) z_m^2 n_p^2 - \left(\mu_p - N_c c(0) - \frac{c(3)}{2} \right) n_p, \end{aligned} \quad (\text{III.13})$$

where we used $2n_I^{\text{Baryon}} = n_B = n_p$ and $\mu_p = \mu_B + \frac{\mu_I}{2}$. Minimizing this in terms of n_p , we have

$$n_p = \frac{2}{g_5^2 z_m^2} \frac{4}{1 + 4N_c^2} \left(\mu_p - c(0) - \frac{c(3)}{2} \right) \quad (\text{III.14})$$

Thus, we set $c(0) + \frac{c(3)}{2} = m_N$ because the proton density n_p must vanish as $\mu_p \rightarrow m_N$.

In Case-(ii), the pion mass depends on not only μ_I but also μ_B through

$$\begin{aligned} E^\pm(\mu_I) &= M \pm \mu_I \left(1 - \frac{1}{1 + 4N_c^2} \frac{z^2}{z_m^2} \right) \\ &\mp 2 \frac{1}{1 + 4N_c^2} (\mu_B - m_N) \frac{z^2}{z_m^2} \mp c(3) \frac{z^2}{z_m^2} \end{aligned} \quad (\text{III.15})$$

in Eq. (III.8). In the limit $\mu_I \rightarrow 0$ at $\mu_B = m_N$ ⁶ the degeneration of the charged pions gives us $c(3) = 0$. The μ_I dependence of the pion mass is the almost same as that in the pure mesonic case (Case-(i)) because the difference is suppressed by the factor $\frac{1}{1 + 4N_c^2} = \frac{1}{37}$.

IV. PION CONDENSATION PHASE

Next, we study the equation of state in the asymmetric nuclear matter. First, we will perform the following analysis in Case-(ii) and in Case-(iii), separately, and show the results of in Case-(iii). In the last of this section, our results on the (μ_I, μ_B) plane will be shown, which are given by combining the result of each Case.

⁵ Note that this definition of the symmetry energy is different from the one used in Ref. [30].

⁶ We can not take the limit $\mu_I \rightarrow 0$ at $\mu_B \neq m_N$ in Case-(ii).

From the Lagrangian Eq. (A.2), the equations of motion are obtained as

$$\begin{aligned}
\partial_5 (-a^3 \partial_5 S^0) + a^3 S^0 (\partial_5 b)^2 - 3a^5 S^0 - a^3 S^0 [\sin^2 b (\varphi^3 + \mu_I)^2 + \theta \sin 2b \sin \zeta (\varphi^3 + \mu_I) + \theta^2 - \theta^2 \sin^2 b \sin^2 \zeta] &= 0, \\
\partial_5 \left(-a^3 (S^0)^2 \partial_5 b \right) - \frac{a^3 (S^0)^2}{2} [\sin 2b \{ (\varphi^3 + \mu_I)^2 - \theta^2 \sin^2 \zeta \} + 2\theta \cos 2b \sin \zeta (\varphi^3 + \mu_I)] &= 0, \\
\partial_5 \left(\frac{a}{g_5^2} \partial_5 \theta \right) - \frac{a}{g_5^2} \theta (\partial_5 \zeta)^2 - \frac{a^3 (S^0)^2}{2} [\sin 2b \sin \zeta (\varphi^3 + \mu_I) + 2\theta \{ 1 - \sin^2 b \sin^2 \zeta \}] &= 0, \\
\partial_5 \left(\frac{a}{g_5^2} \theta^2 \partial_5 \zeta \right) - \frac{a^3 (S^0)^2}{2} [\theta \sin 2b \cos \zeta (\varphi^3 + \mu_I) - \theta^2 \sin^2 b \sin 2\zeta] &= 0, \\
\partial_5 \left(\frac{a}{g_5^2} \partial_5 \varphi^3 \right) - \frac{a^3 (S^0)^2}{2} [2 \sin^2 b (\varphi^3 + \mu_I) + \theta \sin 2b \sin \zeta] &= 0.
\end{aligned} \tag{IV.1}$$

These differential equations are solved with the boundary conditions listed in Table I. We note that, in Case-

Variables	UV	IR
S^0	$\frac{S^0}{z} _\epsilon = m_q$	$\partial_5 S^0 _{z_m} = -\frac{S^0}{2z_m} \left(\lambda (S^0)^2 - 2m^2 \right) _{z_m}$
b	$b _\epsilon = 0$	$\partial_5 b _{z_m} = 0$
θ	$\theta _\epsilon = 0$	$\partial_5 \theta _{z_m} = 0$
ζ	$\zeta _\epsilon = \frac{\pi}{2}$	$\partial_5 \zeta _{z_m} = 0$
φ^3	$\varphi^3 _\epsilon = 0$	$\varphi^3 _{z_m} = -\mu_I$ in Case-(iii) (IR condition) in Case-(ii)

Table I: Boundary conditions for the relevant wave functions. (IR condition) implies that $N_c^2 \partial_5 \varphi^3|_{z_m} + \frac{1}{2} \varphi^3|_{z_m} + \mu_B + \frac{\mu_I}{2} - m_N = 0$ is satisfied.

(iii), the IR boundary condition for φ^3 and the value of n_I^{Baryon} are determined by the minimization condition for the grand potential

$$\begin{aligned}
0 = \frac{\partial \Omega}{\partial n_I^{\text{Baryon}}} &= - \int dz V_0^3 \delta(z - z_m + \delta z) \\
&= -\mu_I - \varphi^3|_{z_m - \delta z}, \tag{IV.2}
\end{aligned}$$

and the condition in Eq. (II.24)

$$n_I^{\text{Baryon}} = -\frac{1}{g_5^2} \frac{\partial_5 \varphi^3}{z} \Big|_{z_m}. \tag{IV.3}$$

In Case-(ii), on the other hand, the condition $\partial \Omega / \partial n_p = 0$ together with the solution of φ^0 and the condition in Eq. (II.24) leads to

$$N_c^2 \partial_5 \varphi^3|_{z_m} + \frac{1}{2} \varphi^3|_{z_m} + \mu_B + \frac{\mu_I}{2} - m_N = 0. \tag{IV.4}$$

It should be noticed that the condition provides the μ_B dependence of the isospin number density n_I in Case-(ii), although the coupled equations of motion in Eq. (IV.1)

do not include μ_B . On the other hand, in Case-(iii), neither the boundary conditions nor the equations of motion have μ_B dependence, which implies that the isospin number density is independent of the baryon number chemical potential.

Now, let us study the isospin number density in Case-(iii), which is defined by

$$n_I = -\frac{\partial \Omega}{\partial \mu_I} = n_I^{\text{Meson}} + n_I^{\text{Baryon}} \tag{IV.5}$$

where the n_I^{Meson} expresses the mesonic contribution to the isospin number density given by

$$n_I^{\text{Meson}} = \int dz \frac{a^3 (S^0)^2}{2} [2 \sin^2 b (\varphi + \mu_I) + \theta \sin 2b \sin \zeta]. \tag{IV.6}$$

In Fig. 2, we show the resultant equation of state between the isospin density and the isospin chemical potential obtained by solving Eq. (IV.1). For $\mu_I < 235$ MeV there is no pion condensation, so that the isospin number density increases linearly with the chemical potential following Eq. (III.3) as drawn by the red curve in Fig. 2. At $\mu_I^c = 235$ MeV the phase transition occurs from the normal hadron phase to the pion condensation phase. This critical chemical potential $\mu_I^c = 235$ MeV is consistent with the one determined from the pion mass shown in Fig. 1, but the value is larger than the critical value for the pure mesonic matter, for which $\mu_I^c = m_\pi$ [22] as seen by the green curve in Fig. 2. This delay of the phase transition is due to the existence of the baryons, which can also be understood by an analysis of the four dimensional chiral Lagrangian as shown in the next section.

In the pion condensation phase, the pion contribution to the isospin number density increases monotonically with the chemical potential as shown by the pink curve in Fig. 2, while the baryonic contribution by the blue curve is almost constant: $n_I^{\text{Baryon}} \sim 0.2 \text{ fm}^{-3}$. As a result the mesonic contribution dominates the isospin number density. This implies that the energy provided by the

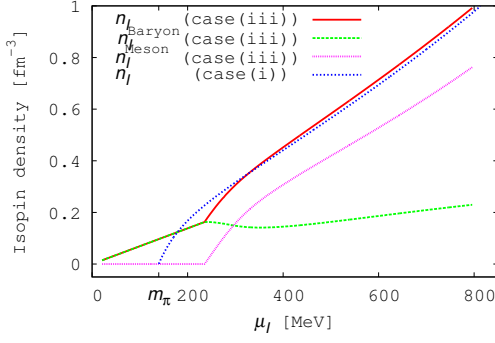


Fig. 2: Equation of state between the isospin chemical potential μ_I and the isospin number density n_I drawn by the red curve. The blue and green curves show the μ_I dependences of the mesonic contribution n_I^{Meson} and the baryonic contribution n_I^{Baryon} , respectively. The pink dots show the result shown in Ref. [22] for pure mesonic matter.

isospin chemical potential is mostly used for generating the pion condensation rather than converting the neutron into proton.

Figure 3 shows the dependence of the equation of state on the scalar meson mass. The value of parameter λ is determined from the mass of the a_0 meson, where $\lambda = 1.0, 4.4$ and 100 correspond to the $m_{a_0} = 610, 980$ and 1210 MeV, respectively. We find that the critical value of the isospin chemical potential is independent of λ and the behavior of the equation of state is not sensitive to the value of λ .

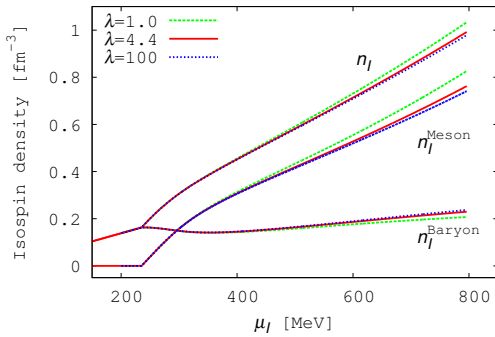


Fig. 3: Dependence of the equation of state on the value of λ . The green, red and blue curves are for $\lambda = 1.0, 4.4$ and 100 , respectively.

As we stated in the introduction, the existence of the isospin chemical potential μ_I explicitly breaks the chiral symmetry group $SU(2)_R \times SU(2)_L$ down to its subgroup $U(1)_R^{(3)} \times U(1)_L^{(3)} = U(1)_V^{(3)} \times U(1)_A^{(3)}$, where the superscript (3) implies that the generator T_3 of $SU(2)$ is used for the $U(1)$ as $\exp[i\theta_V T_3] \in U(1)_V^{(3)}$. For studying the

order parameters for the phase transition, we define the following π -condensate and the “ σ ”-condensate [22]:

$$\begin{aligned} \langle \pi^a \rangle &\equiv \frac{1}{2} \text{Tr} \left[i \sigma^a a \left(\partial_5 \frac{X}{z} \right) + \text{h.c.} \right]_\epsilon = \langle \bar{q} \gamma_5 \sigma^a q \rangle, \\ \langle \sigma \rangle &\equiv \frac{1}{2} \text{Tr} \left[a \left(\partial_5 \frac{X}{z} \right) + \text{h.c.} \right]_\epsilon = \langle \bar{q} q \rangle. \end{aligned} \quad (\text{IV.7})$$

We plot the “ σ ”-condensate and the π -condensate obtained by the present analysis in Fig. 4, together with those condensates for the pure mesonic matter. This fig-

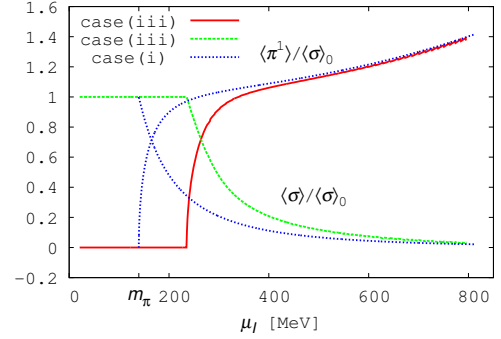


Fig. 4: Dependence of the “ σ ”-condensate $\langle \sigma \rangle$ and the π -condensate $\langle \pi \rangle$ on the isospin chemical potential μ_I . The condensates are scaled by the “ σ ”-condensate at the vacuum indicated by $\langle \sigma \rangle_0$. The blue curves are the dependence of $\langle \sigma \rangle$ and $\langle \pi \rangle$ shown in Ref. [22] for the pure mesonic matter.

ure shows that the present behavior is quite similar to the previous one except the difference of the phase transition point: In the normal hadron phase the “ σ ”-condensate exists, which leads to the break down of the $U(1)_A^{(3)}$ symmetry, but π -condensate is zero. At the phase transition point, the π -condensate appears, which spontaneously breaks the $U(1)_V^{(3)}$ symmetry, while the “ σ ”-condensate starts to decrease very rapidly. For large μ_I , the “ σ ”-condensate is almost zero while the π -condensate keeps increasing.

We next show the chiral circle in Fig. 5. The red solid curve shows that the behavior for the nuclear matter is quite similar to the one for the pure mesonic matter shown by the green dotted line: Although the “ σ ”-condensate decreases and the π -condensate increases, the chiral condensate defined by

$$\tilde{\sigma} \equiv \sqrt{\langle \sigma \rangle^2 + \langle \pi^a \rangle^2} \quad (\text{IV.8})$$

stays constant until about 150 MeV above the critical chemical potential. In the large μ_I region, the chiral condensate $\tilde{\sigma}$ grows very rapidly. This implies that the enhancement of the chiral symmetry breaking occurs in the asymmetric nuclear matter, similarly to the one in the pure mesonic matter as shown in Ref. [22].

Next, we study the equation of state and the condensates in Case-(ii) as well as those in Case-(i) in a similar way. The resultant $\langle \pi^1 \rangle$, $\langle \sigma \rangle$ and n_I in the entire

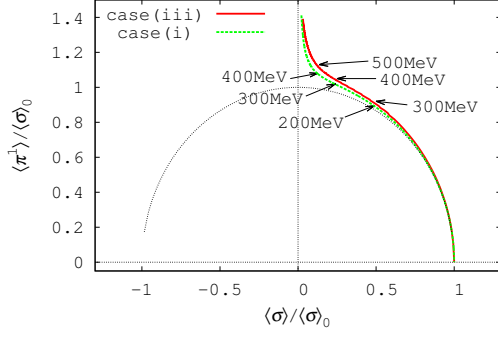


Fig. 5: Chiral circle shown by red curve. The black curve is an unit circle and the green curve is the chiral circle for the pure mesonic matter.

(μ_B, μ_I) plane are shown in Fig. 6, 7 and 8, respectively. The green lines in these figures show the boundary between Case-(i) and Case-(ii) and that between Case-(ii) and Case-(iii), which are corresponding to $\mu_p = m_N$ and $\mu_n = m_N$. Figure 6 shows that there is the first order transition on the boundary between the pion condensation phase in Case-(ii) and the normal hadron phase in Case-(iii). In Fig. 7, we see that $\langle \sigma \rangle$ decreases discontinuously at the first order transition line in response to sudden increase of $\langle \pi^1 \rangle$ in Fig. 6. Figure 8 shows the equation of state on the (μ_B, μ_I) plane. In these figures, the values of $\langle \pi^1 \rangle$, $\langle \sigma \rangle$ and n_I drastically change on $\mu_n = m_N$ which is the boundary between Case-(ii) and Case-(iii).

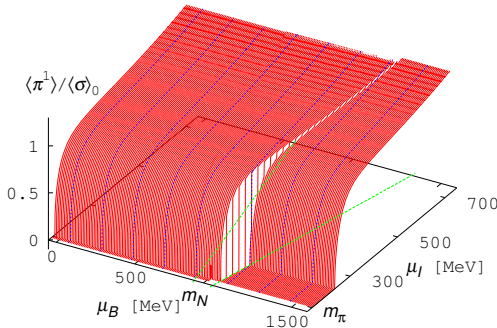


Fig. 6: $\langle \pi^1 \rangle / \langle \sigma \rangle_0$ vs. μ_B vs. μ_I . The green lines are the boundaries between Case-(i) and Case-(ii) and between Case-(ii) and Case-(iii).

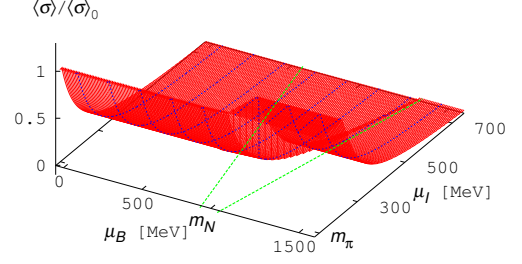


Fig. 7: $\langle \sigma \rangle / \langle \sigma \rangle_0$ vs. μ_B vs. μ_I . The green lines are the boundaries between Case-(i) and Case-(ii) and between Case-(ii) and Case-(iii).

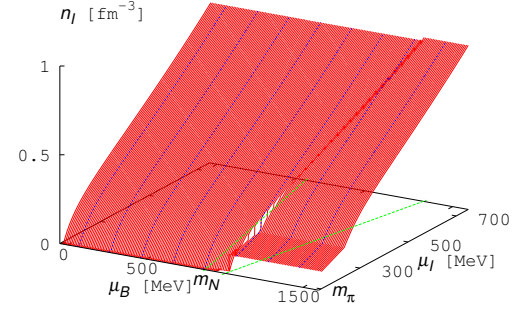


Fig. 8: n_I vs. μ_B vs. μ_I . The green lines are the boundaries between Case-(i) and Case-(ii) and between Case-(ii) and Case-(iii).

V. AN ANALYSIS BY THE CHIRAL LAGRANGIAN BASED ON THE HIDDEN LOCAL SYMMETRY

In this section, we show that the delay of the phase transition to the pion condensation phase is understood as the baryonic matter effect in the framework of the four dimensional chiral Lagrangian including the ρ meson based on the hidden local symmetry (HLS) [25, 26].

The mesonic part of the HLS Lagrangian is given by

$$\begin{aligned} \mathcal{L} = & F_\pi^2 \text{Tr} [\hat{\alpha}_\perp \mu \hat{\alpha}_\perp^\mu] + a F_\pi^2 \text{Tr} [\hat{\alpha}_\parallel \mu \hat{\alpha}_\parallel^\mu] \\ & + \frac{F_\pi^2}{4} \text{Tr} [\xi_L \chi \xi_R^\dagger + \xi_R \chi^\dagger \xi_L] - \frac{1}{2g^2} \text{Tr} [V_{\mu\nu} V^{\mu\nu}] \end{aligned} \quad (\text{V.1})$$

where χ is an external field which has the expectation value corresponding to the pion mass, $\langle \chi \rangle = m_\pi^2 \mathbf{1}$. The

$\hat{\alpha}_{\perp\mu}$ and $\hat{\alpha}_{\parallel\mu}$ are defined as

$$\hat{\alpha}_{\perp,\parallel\mu} = \frac{D_\mu \xi_L \cdot \xi_L^\dagger \pm D_\mu \xi_R \cdot \xi_R^\dagger}{2i} \quad (\text{V.2})$$

where $\xi_{L,R}$ are the fields including pions, V_μ is the gauge field including the rho and omega mesons and the covariant derivative of these fields are

$$\begin{aligned} D_\mu \xi_L &= \partial_\mu \xi_L - iV_\mu \xi_L + i\xi_L \mathcal{L}_\mu, \\ D_\mu \xi_R &= \partial_\mu \xi_R - iV_\mu \xi_R + i\xi_R \mathcal{R}_\mu. \end{aligned} \quad (\text{V.3})$$

The baryon and isospin chemical potentials, μ_B and μ_I , are introduced as the expectation value of the time component of the external gauge fields: $\langle \mathcal{L}_0 \rangle = \langle \mathcal{R}_0 \rangle = \frac{\mu_B}{2} \sigma^0 + \frac{\mu_I}{2} \sigma^3$.

Here we introduce the following terms including the baryons explicitly:

$$\bar{N} i \gamma^\mu D_\mu N + G \bar{N} \gamma^\mu \hat{\alpha}_{\parallel\mu} N \quad (\text{V.4})$$

where N is the baryon field and D_μ is a covariant derivative defined as $D_\mu N = (\partial_\mu - iV_\mu) N$. We replace the bilinear baryon fields by the mean field as

$$\left(V_0^3 + G \hat{\alpha}_{\parallel 0}^3 \right) n_I^{\text{Baryon}} + \left(V_0^0 + G \hat{\alpha}_{\parallel 0}^0 \right) n_B \quad (\text{V.5})$$

where $\hat{\alpha}_{\parallel 0}^{(0,3)} = \text{Tr}(\hat{\alpha}_{\parallel 0} \sigma^{(0,3)})$, V_0^3 is the time component of the neutral rho meson and V_0^0 is the time component of the omega meson.

Taking the unitary gauge of the HLS and integrating out the rho and omega mesons and assuming the rotational symmetry, we obtain the following effective Lagrangian for the pion coupling to the baryonic sources:

$$\begin{aligned} \mathcal{L} &= F_\pi^2 \text{Tr}[\hat{\alpha}_{\perp 0} \hat{\alpha}_{\perp}^0] + \frac{F_\pi^2}{4} \text{Tr}[\xi_L \chi \xi_R^\dagger + \xi_R \chi^\dagger \xi_L] \\ &\quad - \frac{1}{2a' F_\pi^2} n_B^2 - \frac{1}{2a' F_\pi^2} \left(n_I^{\text{Baryon}} \right)^2 + \mu_B n_B + \alpha_{\parallel 0}^3 n_I^{\text{Baryon}} \end{aligned} \quad (\text{V.6})$$

where $a' \equiv \frac{a}{(1-G)^2}$ ⁷ and $\alpha_{\parallel}^\mu = \hat{\alpha}_{\parallel}^\mu + V^\mu$. Existence of the terms in the last line of Eq. (V.6) causes the deviation from the result obtained by the $\mathcal{O}(p^2)$ chiral Lagrangian without the baryonic sources, which delays the transition to the pion condensation comparing to of the pure mesonic analysis. Figure 9 shows the relation between the pion mass and the isospin chemical potential for $a' = 0.7$ (green), 0.5 (blue), 0.3 (pink) and of the holographic QCD model (the red curve). The dotted black line corresponds to the case for the pure pion matter, $a' = 0$. This figure shows that the point at which the

curve reaches zero depends on the value of a' . The critical value of the isospin chemical potential for $0 < a' < 1$ is larger than the pion mass, which implies that delay of the transition is understood by using a model based on the HLS with the baryonic sources.

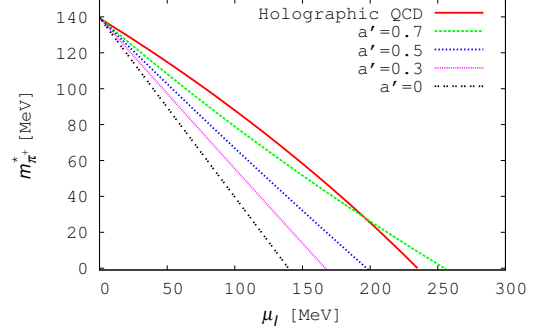


Fig. 9: The μ_I dependence of the π^+ mass obtained from the chiral Lagrangian. The green, blue and pink curves are the results for $a' = 0.7, 0.5$ and 0.3 respectively. The π^+ mass given from the analysis of the holographic QCD model is indicated by the red curve. We also show the μ_I dependence of the π^+ mass in the pure mesonic matter obtained in Ref. [22] by the dotted black line.

VI. A SUMMARY AND DISCUSSIONS

We introduced a baryonic source at the IR boundary coupling to the iso-triplet vector meson in the hard wall holographic QCD mode, and studied the pion condensation in the asymmetric nuclear matter. We showed that the phase transition from the normal matter to the pion condensation phase is delayed in the asymmetric nuclear matter compared with the pure mesonic matter. Furthermore, our result shows that the meson contribution to the isospin number density increases with the chemical potential, while the baryon contribution stays constant. We would like to stress that the chiral symmetry breaking is enhanced in the asymmetric nuclear matter as in the pure mesonic matter.

We show the phase diagram obtained from the present analysis in Fig. 10, where the blue and red area express the hadron phase and the pion condensation phase respectively. The phase transition is of the second order except on the yellow line expressing the first order. In Case-(i), the phase transition to the pion condensation occurs at which the isospin chemical potential is equal to the pion mass as shown in Ref. [22]. On the other hand, in Case-(iii), done by the present analysis, the critical point of the transition is delayed compared with in Case-(i). A similar delay also occurs in Case-(ii), although the effect is very tiny and it is hard to see in Fig. 10.

The model which we used in section V explicitly includes the rho and omega mesons. The existence of the

⁷ Since the value of the parameter a is known as about two in the HLS [26], $a' = \frac{a}{(1-G)^2}$ is larger than zero.

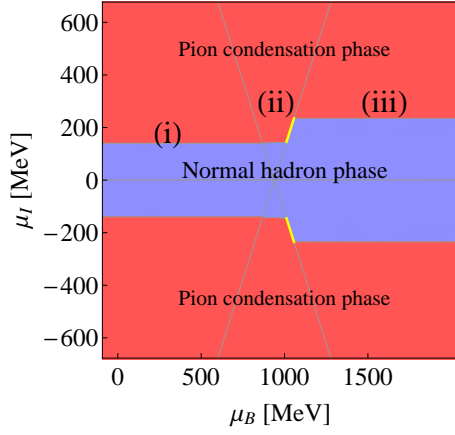


Fig. 10: Phase diagram: μ_B vs. μ_I . The blue and red area express the hadron phase and the pion condensation phase respectively.

rho meson is essential for the delay of the phase transition. This indicate that the phase transition point in the NJL model may be changed by including the following vector 4-Fermi interaction [14, 34–38]:

$$g_v \left[(\bar{\psi} \sigma^a \gamma_\mu \psi)^2 + (\bar{\psi} \sigma^a \gamma_\mu \gamma_5 \psi)^2 \right] \quad (\text{VI.1})$$

where g_v is a positive coupling constant, ψ is a quark field and σ^a are Pauli matrices in the flavor space.

In the present analysis, we put the baryonic charge at the IR boundary. In more general case, the charge is spread into the bulk by the gauge interaction. Furthermore, the coupling of the baryon to the scalar mesons is not included. Such effects could be included by the holographic mean field approach [39, 40], which is left

for future publication.

References [16, 30, 41] studied the asymmetric matter in the hard wall holographic QCD model. Our results for the meson mass splitting and the symmetry energy are comparable to their results.

ACKNOWLEDGEMENTS

The authors would like to thank Kenji Fukushima for stimulating discussion on the symmetry structure. This work was supported in part by Grant-in-Aid for Scientific Research on Innovative Areas (No. 2104) “Quest on New Hadrons with Variety of Flavors” from MEXT, and the JSPS Grant-in-Aid for Scientific Research (S) No. 22224003, (c) No. 24540266.

Appendix A: Equations of motion

At the vacuum, non zero value of S^0 brakes the chiral symmetry to the vector part of its symmetry. The iso-singlet scalar field S^0 satisfies the following equation of motion (EOM) and the boundary conditions:

$$\begin{aligned} \partial_5 a^3 \partial_5 S^0 + 3a^5 S^0 &= 0, \\ m_q &= \left. \frac{S^0}{z} \right|_\epsilon, \\ \left[\partial_5 S^0 + \frac{S^0}{2z_m} \left(\lambda (S^0)^2 - 2m^2 \right) \right]_{z_m} &= 0 \end{aligned} \quad (\text{A.1})$$

where the m_q corresponds to the explicit braking of the chiral symmetry due to the current quark mass.

Using the assumptions given in section II and the variables parameterized in Eqs. (II.12) and (II.13), the Lagrangian \mathcal{L} is written as

$$\begin{aligned} \mathcal{L} &= \mathcal{L}_1 + \mathcal{L}_2, \\ \mathcal{L}_1 &= \frac{a^3}{2} \left[-(\partial_5 S^0)^2 - (S^0)^2 (\partial_5 b)^2 \right] + \frac{3a^5}{2} (S^0)^2 \\ &\quad + \frac{a^3 (S^0)^2}{2} \left[\sin^2 b (V_0^3)^2 + \theta \sin 2b \sin \zeta V_0^3 + \theta^2 - \theta^2 \sin^2 b \sin^2 \zeta \right] \\ &\quad + \frac{a}{2g_5^2} \left[(\partial_5 V_0^3)^2 + (\partial_5 \theta)^2 + \theta^2 (\partial_5 \zeta)^2 \right] + \rho_I V_0^3 \delta(z - z_m + \delta z), \\ \mathcal{L}_2 &= \frac{a}{2g_5^2} (\partial_5 V_0^0)^2 + \rho_q V_0^0 \delta(z - z_m + \delta z) \end{aligned} \quad (\text{A.2})$$

where

$$\begin{aligned} e^{i\pi^a \sigma^a} &= \cos b + i \sin b \sigma^1, \\ A_0^a &= (\theta \cos \zeta, \theta \sin \zeta, 0). \end{aligned} \quad (\text{A.3})$$

For convenience, we fixed $\pi^2 = 0$ by using the isospin symmetry $U(1)_I$ which is the subgroup of $U(1)_L^3 \times U(1)_R^3$.

-
- [1] See, e.g. J. M. Lattimer and M. Prakash, Phys. Rept. **442**, 109 (2007) and references therein.
 - [2] P. Demorest, T. Pennucci, S. Ransom, M. Roberts and J. Hessels, Nature **467**, 1081 (2010).
 - [3] J. Antoniadis, P. C. C. Freire, N. Wex, T. M. Tauris, R. S. Lynch, M. H. van Kerkwijk, M. Kramer and C. Bassa *et al.*, Science **340**, 6131 (2013).
 - [4] K. Fukushima and T. Hatsuda, Rept. Prog. Phys. **74**, 014001 (2011).
 - [5] K. Fukushima and C. Sasaki, Prog. Part. Nucl. Phys. **72**, 99 (2013).
 - [6] T. Sasaki, Y. Sakai, H. Kouno and M. Yahiro, Phys. Rev. D **82**, 116004 (2010).
 - [7] Z. Zhang and Y. X. Liu, Phys. Rev. C **75**, 064910 (2007).
 - [8] D. Toublan and J. B. Kogut, Phys. Lett. B **564**, 212 (2003).
 - [9] A. Barducci, R. Casalbuoni, G. Pettini and L. Ravagli, Phys. Rev. D **69**, 096004 (2004).
 - [10] L. y. He, M. Jin and P. f. Zhuang, Phys. Rev. D **71**, 116001 (2005).
 - [11] C. f. Mu, L. y. He and Y. x. Liu, Phys. Rev. D **82**, 056006 (2010).
 - [12] L. He, M. Jin and P. Zhuang, Phys. Rev. D **74**, 036005 (2006).
 - [13] L. y. He, M. Jin and P. f. Zhuang, Mod. Phys. Lett. A **22**, 637 (2007).
 - [14] Z. Zhang and H. P. Su, Phys. Rev. D **89**, 054020 (2014).
 - [15] J. O. Andersen and L. Kyllingstad, J. Phys. G **37**, 015003 (2009).
 - [16] B. -H. Lee, S. Mamedov, S. Nam and C. Park, JHEP **1308**, 045 (2013).
 - [17] A. Parnachev, JHEP **0802**, 062 (2008).
 - [18] B. Klein, D. Toublan and J. J. M. Verbaarschot, Phys. Rev. D **68**, 014009 (2003).
 - [19] Y. Nishida, Phys. Rev. D **69**, 094501 (2004).
 - [20] D. Toublan and J. B. Kogut, Phys. Lett. B **605**, 129 (2005).
 - [21] H. Abuki, Phys. Rev. D **87**, 094006 (2013).
 - [22] H. Nishihara and M. Harada, Phys. Rev. D **89**, 076001 (2014).
 - [23] D. T. Son and M. A. Stephanov, Phys. Rev. Lett. **86**, 592 (2001).
 - [24] K. -Y. Kim, S. -J. Sin and I. Zahed, JHEP **0801**, 002 (2008).
 - [25] M. Bando, T. Kugo and K. Yamawaki, Phys. Rept. **164**, 217 (1988).
 - [26] M. Harada and K. Yamawaki, Phys. Rept. **381**, 1 (2003).
 - [27] J. Erlich, E. Katz, D. T. Son and M. A. Stephanov, Phys. Rev. Lett. **95**, 261602 (2005).
 - [28] L. Da Rold and A. Pomarol, Nucl. Phys. B **721**, 79 (2005).
 - [29] L. Da Rold and A. Pomarol, JHEP **0601**, 157 (2006).
 - [30] C. Park, Phys. Lett. B **708**, 324 (2012).
 - [31] Z. Zhang and L. -W. Chen, Phys. Lett. B **726**, 234 (2013).
 - [32] L. -W. Chen, C. M. Ko and B. -A. Li, Phys. Rev. Lett. **94**, 032701 (2005).
 - [33] D. V. Shetty, S. J. Yennello and G. A. Souliotis, Phys. Rev. C **76**, 024606 (2007) [Erratum-ibid. C **76**, 039902 (2007)].
 - [34] M. Asakawa and K. Yazaki, Nucl. Phys. A **504**, 668 (1989).
 - [35] M. Kitazawa, T. Koide, T. Kunihiro and Y. Nemoto, Prog. Theor. Phys. **108**, 929 (2002).
 - [36] K. Fukushima, Phys. Rev. D **78**, 114019 (2008).
 - [37] Z. Zhang and T. Kunihiro, Phys. Rev. D **80**, 014015 (2009).
 - [38] N. M. Bratovic, T. Hatsuda and W. Weise, Phys. Lett. B **719**, 131 (2013).
 - [39] M. Harada, S. Nakamura and S. Takemoto, Phys. Rev. D **86**, 021901 (2012).
 - [40] B. -R. He and M. Harada, Phys. Rev. D **88**, no. 9, 095007 (2013).
 - [41] K. Jo, B. -H. Lee, C. Park and S. -J. Sin, JHEP **1006**, 022 (2010).